

# A Nonlinear Least-Squares Solution with Causality Constraints Applied to Transmission Line Permittivity and Permeability Determination

James Baker-Jarvis, Richard G. Geyer, and Paul D. Domich

**Abstract**—A technique for the solution of 1-port and 2-port scattering equations for complex permittivity and permeability determination is presented. Using a nonlinear regression procedure, the model determines parameters for the specification of the spectral functional form of complex permittivity and permeability. The method is based on a nonlinear regression technique using the fact that a causal, analytic function can be represented by poles and zeros. The technique allows the accurate determination of many low- and high-permittivity dielectric or magnetic materials in either the low- or high-loss range. Permeability and permittivity can be obtained either from fitting all scattering-parameter data or by fitting  $S_{21}$  or  $S_{11}$  or  $|S_{11}|$  and  $|S_{21}|$  data by itself. The model allows for small adjustments, consistent with the physics of the problem, to independent variable data such as angular frequency, sample length, sample position, and cutoff wavelength. The model can determine permittivity and permeability for samples where sample length, sample position, and sample holder length are not known precisely. The problem of local minima is discussed.

**Keywords**—Dielectric measurements, higher order modes, microwave, orthogonal distance regression, permeability, permittivity, primary mode.

## I. INTRODUCTION

COMBINED permeability and permittivity determination using transmission line fixtures has been studied extensively over the years [1]–[6]. The theory underlying linear  $n$ -ports for inverse scattering problems has been worked out decades ago. Since then numerical strategies have been employed in the reduction of 1-port and 2-port scattering data for both nonmagnetic and magnetic materials. The vast majority of the work in this area has involved the determination of permittivity and permeability by the reduction of scattering data on a frequency-by-frequency or point-by-point basis, that is, by the explicit or implicit solution of a system of nonlinear scattering

equations at each particular frequency. (See [2]–[4]. As an example of a multifrequency approach see [5].) What is lacking in the literature are practical, robust, numerical reduction techniques for accurate determination of permittivity and permeability in transmission lines. Reliable broadband permeability and permittivity results for low-loss, medium-to-high dielectric constant materials are hard to obtain with transmission line techniques. Coaxial line measurements are particularly hard to obtain due to the effects of air gaps and overmoding. Traditional transmission line numerical techniques have difficulties to the extent that they render these techniques of limited use for low-loss materials and for high dielectric constant materials.

Difficulties arise with these methods for magnetic materials in that numerical singularities can occur at frequencies corresponding to integral multiples of one-half wavelength. These instabilities arise from the fact that in the limit of very low loss at frequencies corresponding to one-half wavelength in the material, both  $S_{21}$  and  $S_{11}$  reduce to equations for determination of the phase velocity only. In this limit the permittivity and permeability therefore enter as a product. In point-by-point short-circuit line or open-circuit line 1-port measurement techniques, either measurements on two samples or two positions must be obtained. This is problematic since samples are often slightly inhomogeneous and cannot be machined in a totally reproducible manner. There also are uncertainties in locating the positions precisely for two-position measurements. Another problem pertains to high-dielectric constant materials. High dielectric constant materials are usually hard to measure since the theoretical models are limited to a single, fundamental mode; however, the data contain both fundamental and higher mode responses. Imperfections in either the sample or sample holder promote mode conversion from the fundamental mode into higher modes. These generated higher modes propagate only in the sample and are evanescent outside. Evidence of the existence of the higher modes becomes apparent at resonant frequencies of the modes where the sample acts as resonant cavity. At these frequencies there is a noticeable dip in the  $S_{11}$  parameter due to resonant absorption.

Manuscript received August 30, 1992; revised February 20, 1992.

J. Baker-Jarvis and R. G. Geyer are with the Electromagnetic Fields Division, National Institute of Standards and Technology, Boulder, CO 80303-3328.

P. D. Domich is with the Applied and Computational Mathematic Division, National Institute of Standards and Technology, Boulder, CO 80303-3328.

IEEE Log Number 9202170.

Point-by-point reduction techniques for magnetic materials contain large random uncertainties due to the propagation of uncertainties through the equations. For non-magnetic materials the propagation of errors is less of a problem.

In our search for better reduction techniques we have found that nonlinear processes, which minimize the square error, are a viable alternative solution. Optimization-based data reduction has an advantage over point-by-point schemes in that correlations are allowed between frequency measurements. In nonlinear regression, if deemed appropriate, it is not necessary to even include  $S_{11}$  in the set of constraint equations. Another advantage of regression is that constraints such as causality and positivity can be incorporated into the solution.

This paper presents a method for obtaining complex permittivity and permeability spectra from scattering-parameter data on isotropic, homogeneous materials using a nonlinear regression model. We solve the scattering equations in a nonlinear least-squares sense with a regression algorithm over the entire frequency measurement range. The complex permittivity and permeability are obtained by determining estimates for the coefficients of a pole-zero model for these parameters consistent with linearity and causality constraints. The procedure has been successfully used for accurate permittivity and permeability characterization of a number of different samples where point-by-point schemes have been found to be inadequate. The details of the numerical method have been presented elsewhere [6]. The problem applied to microwave measurements is presented in this paper. The method can be extended to the analysis of multimode problems and the determination of experimental systematic uncertainty. The novel features of our algorithm are summarized below.

- The algorithm finds a ‘‘best fit’’ to the scattering equations using a Levenburg-Marquardt nonlinear least-squares solution for the permittivity and permeability.
- The algorithm uses fitting functions that satisfy causality and energy requirements.
- The numerical technique allows slight variations in the sample and reference position lengths to compensate for measurement errors.
- The method allows the deemphasis of frequency points with large phase uncertainty.
- Statistics related to the solution parameters are automatically generated.
- The technique can force positivity of the fit functions.
- It is possible to determine both complex permittivity and permeability from measurements of a single scattering parameter on a 1-port or a 2-port taken over a frequency band.

## II. SCATTERING PARAMETER RELATIONS

In the scattering formalism we develop in this section we assume that the primary modes in the transmission line

are TEM for coaxial line and  $TE_{01}$  for waveguide. In the analysis that follows we assume  $\exp(j\omega t)$  time dependence.

The complex permittivity is

$$\epsilon = [\epsilon'_R - j\epsilon''_R]\epsilon_o = \epsilon_R^*\epsilon_o \quad (1)$$

and the complex permeability is

$$\mu = [\mu'_R - j\mu''_R]\mu_o = \mu_R^*\mu_o. \quad (2)$$

Here  $\epsilon_o$  and  $\mu_o$  are the permittivity and permeability of vacuum, and  $\epsilon_R^*$  and  $\mu_R^*$  are the relative complex permittivity and permeability relative to air in the laboratory. The propagation constant in the material is

$$\gamma = j\sqrt{\frac{\omega^2\mu_R^*\epsilon_R^*}{c_{vac}^2} - \left(\frac{2\pi}{\lambda_c}\right)^2} \quad (3)$$

and in air

$$\gamma_o = j\sqrt{\left(\frac{\omega}{c_{lab}}\right)^2 - \left(\frac{2\pi}{\lambda_c}\right)^2} \quad (4)$$

where  $\lambda_c$  is the cutoff wavelength in the waveguide measurement fixture in air,  $c_{vac}$  and  $c_{lab}$  are the speed of light in vacuum and the laboratory, respectively, and  $\omega = 2\pi f$ . The expression for the transmission coefficient  $z$  can be formed in terms of the propagation constant

$$z = \exp(-\gamma L), \quad (5)$$

where  $L$  is the sample length. A reflection parameter can be defined as

$$\Gamma = \frac{\frac{\mu}{\mu_o}\gamma_o - 1}{\frac{\mu}{\mu_o}\gamma_o + 1} \quad (6)$$

for coaxial line  $1/\lambda_c \rightarrow 0$ . It is assumed that the total length of the sample holder is

$$L_{air} = L + L_1 + L_2 \quad (7)$$

where  $L$  is the sample length, and  $L_1$  and  $L_2$  are the distances from the calibration reference planes to the sample faces, as indicated in Fig. 1. We assume that  $L_{air}$  and  $L$  are known to high accuracy, but  $L_1$  and  $L_2$  may not be known precisely.

For a two-port device, the expressions for the measured scattering parameters are obtained by solving a related boundary value problem [7]. The transformation of the scattering matrix ( $\bar{S}$ ) to the sample face requires a linear transformation

$$\bar{S}' = \bar{\Phi}\bar{S}\bar{\Phi} \quad (8)$$

where

$$\bar{\Phi} = \begin{pmatrix} \exp(-\gamma_o L_1) & 0 \\ 0 & \exp(-\gamma_o L_2) \end{pmatrix}. \quad (9)$$

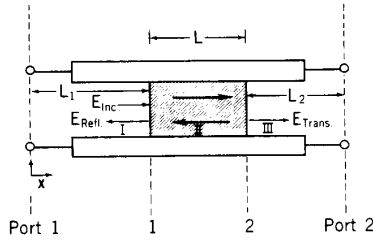


Fig. 1. A dielectric sample in a transmission line with regions I, II, and III denoted. Port 1 and port 2 denote calibration reference plane positions.

The explicit expressions for the fundamental mode 2-port scattering relations are given by

$$S_{11}(\lambda_c) = R_1^2 \left[ \frac{\Gamma(1 - z^2)}{1 - \Gamma^2 z^2} \right] \quad (10)$$

$$S_{21}(\lambda_c) = R_1 R_2 \left[ \frac{z(1 - \Gamma^2)}{1 - \Gamma^2 z^2} \right] = S_{12}(\lambda_c) \quad (11)$$

$$S_{22}(\lambda_c) = R_2^2 \left[ \frac{\Gamma(1 - z^2)}{1 - \Gamma^2 z^2} \right] \quad (12)$$

where the scattering matrix is assumed to be measured at the calibration plane. The reciprocity in (11) requires isotropic and demagnetized materials. Also

$$R_1 = \exp(-\gamma_0 L_1) \quad (13)$$

and

$$R_2 = \exp(-\gamma_0 L_2) \quad (14)$$

are rotation terms.

Another useful expression is the determinant of the scattering matrix:

$$S_{11} S_{22} - S_{12} S_{21} = \exp[(-2\gamma_0)(L_{\text{air}} - L)] \frac{\Gamma^2 - z^2}{1 - \Gamma^2 z^2}. \quad (15)$$

The problem is to determine the complex permittivity and permeability from (10)–(12) or (15). We use various combinations of (11)–(15) in our numerical methods.

For 1-port measurements the following equation is used in the model [7]:

$$S_{11} = \frac{\tanh \gamma L + \Theta \tanh \gamma_0 \Delta L - \Theta(1 + \Theta \tanh \gamma L \tanh \gamma_0 \Delta L)}{\tanh \gamma L + \Theta \tanh \gamma_0 \Delta L + \Theta(1 + \Theta \tanh \gamma L \tanh \gamma_0 \Delta L)} \quad (16)$$

where

$$\Theta = \frac{\gamma \mu_o}{\gamma_o \mu} \quad (17)$$

and  $\Delta L$  is the distance from the back face of the sample to the short-circuit termination.

### III. MODEL FOR PERMEABILITY AND PERMITTIVITY DETERMINATION

Viewed from a formal aspect the unknown quantities are  $L_1$ ,  $L_2$ ,  $L$ ,  $\lambda_c$ ,  $\mu_R^*(\omega)$ , and  $\epsilon_R^*(\omega)$ . Some of these param-

eters, such as the lengths and cutoff wavelength, are known accurately within the measurement uncertainty of a measurement device.

Since it is not computationally feasible to treat all of the permittivities and permeabilities at all the measured frequencies as unknown quantities, the numerical model uses an explicit frequency-dependent form for  $\mu_R^*$  and  $\epsilon_R^*$ . The general form for  $\mu_R^*(\omega)$  and  $\epsilon_R^*(\omega)$  should be causal; that is, it should satisfy a Kramers–Kronig relation. The zeros and poles of a complex function determine the function.

The Laplace transform of the real, time-dependent permittivity satisfies

$$\epsilon(\vec{r}, s) = \int_0^\infty \epsilon(\vec{r}, t) e^{-st} dt. \quad (18)$$

For stability there can be no poles in the right half of the  $s$ -plane. Since  $\epsilon(t)$  is real it can be shown that the poles and zeros are confined to the negative real  $s$ -axis of the  $s$ -plane, and the poles which are off the real  $s$ -axis must occur in complex conjugate pairs [8].

The Debye model for materials uses the following expression for permittivity:

$$\epsilon_R^* = \frac{A}{1 + jB\omega} + C. \quad (19)$$

In our present algorithm we use two approaches, the first for magnetic materials and the second for nonmagnetic materials. In the first model a series of poles of first and second order is assumed for  $\mu_R^*(\omega)$  and  $\epsilon_R^*(\omega)$ . This expansion

$$\mu_R^*(\omega) = A_0 + \sum_i \frac{A_{1i}}{1 + jB_{1i}\omega} + \sum_i \frac{A_{2i}}{(1 + jB_{2i}\omega)^2}, \quad (20)$$

$$\epsilon_R^*(\omega) = D_0 + \sum_i \frac{A_{3i}}{1 + jB_{3i}\omega} + \sum_i \frac{A_{4i}}{(1 + jB_{4i}\omega)^2} \quad (21)$$

has generally yielded excellent results, where  $B_i$  are real numbers. The poles should all reside in the left half-plane. In the algorithm a couple of poles per frequency decade is assumed.

The second model is used for dielectric materials:

$$\epsilon_R^* = C \prod_n \frac{(j\omega + z_n)}{(j\omega + p_n)}. \quad (22)$$

Here  $z_n$  and  $p_n$  are the zeros and poles.

For a typical measurement on a network analyzer there may be 400 frequency points, and at each all four scattering parameters ( $S$ -parameters) are obtained (although, in practice, since within measurement error,  $S_{21} = S_{12}$ , there are only three independent parameters). The problem is overdetermined since for  $n$  frequency measure-

ments, there are (assuming lengths to be known accurately)  $6n$  real equations for the handful of unknown pole-zero quantities.

For more complicated polarization phenomena other relations for permittivity could be used:

$$\epsilon' = \epsilon_\infty + [\epsilon(0) - \epsilon_\infty] \int_0^\infty \frac{y(\tau)}{1 + \omega^2 \tau^2} d\tau \quad (23)$$

$$\epsilon'' = [\epsilon(0) - \epsilon_\infty] \int_0^\infty \frac{\omega \tau y(\tau)}{1 + \omega^2 \tau^2} d\tau \quad (24)$$

where  $y(\tau)$  is a distribution function. It is possible to expand this distribution in terms of moments:

$$\begin{aligned} \epsilon' - j\epsilon'' &= \epsilon_\infty + [\epsilon(0) - \epsilon_\infty] \sum_{n=0}^{\infty} \int_0^\infty (j\omega\tau)^n y(\tau) d\tau \\ &= \epsilon_\infty + [\epsilon(0) - \epsilon_\infty] \sum_{n=0}^{\infty} \int_0^\infty y(\tau) (j)^n \tau^n \omega^n d\tau \end{aligned} \quad (25)$$

$$\begin{aligned} &= \epsilon_\infty + [\epsilon(0) - \epsilon_\infty] \sum_{n=0,2,4,\dots}^{\infty} (-1)^n \langle y^n \rangle \omega^n \\ &\quad - j(-1)^n [\epsilon(0) - \epsilon_\infty] \sum_{n=1,3,\dots}^{\infty} \langle x^n \rangle \omega^n \end{aligned} \quad (26)$$

where

$$\langle y^n \rangle = \int_0^\infty \tau^n y(\tau) d\tau. \quad (27)$$

Therefore, the real part of the permittivity is an expansion in terms of the even moments, and the odd part of the permittivity is an expansion in terms of the odd moments. The moments which promote a least-squares fit may be found by the optimization routine. We currently use (20)–(22) in our calculations.

The approach for determining the parameters  $A_j$  and  $B_j$  is to minimize the sum of the squares of the differences between the predicted and observed  $S$ -parameters,

$$\min \left\| \sum_{ij} \vec{S}_{ij} - \vec{P}_{ij} \right\|, \quad (28)$$

where the measured vectors are denoted by  $\vec{S}_{ij} = (S_{ij}(\omega_1), S_{ij}(\omega_2), \dots, S_{ij}(\omega_n))$  and where  $\vec{P}_{ij}$  is the predicted  $S$ -parameter vector. Hence, the problem is of finding the minimum normal solution to these equations.

#### IV. NUMERICAL TECHNIQUE

##### A. Numerical Algorithm

The solution currently uses a software routine called ODRPACK (orthogonal distance regression pack) [9] developed at the National Institute of Standards and Technology. This routine is an extended form of the Levenberg-Marquardt approach. This procedure allows for both

ordinary nonlinear least-squares, in which the uncertainties are assumed to be only in the dependent variable, and orthogonal distance regression, where the uncertainties appear in both dependent and independent variables. First-order derivatives for the Jacobian matrices can be numerically approximated (finite difference approximation), or can be user-supplied analytical derivatives. The procedure performs automatic scaling of the variables if necessary, as well as determining the accuracy of the model in terms of machine precision. The trust region approach enables the procedure to adaptively determine the region in which the linear approximation adequately represents the nonlinear model.

Iterations are stopped by ODRPACK when any one of three criteria is met. These criteria are: 1) the difference between observed and predicted values is small, 2) the convergence to a predicted value is sufficiently small, and 3) a specified limit on the number of iterations has been reached.

Initial estimates for  $\epsilon_R^*$  and  $\mu_R^*$  are obtained from explicit solutions [1], [10]. The most significant input parameters for modeling permittivity and permeability are the initial values for  $A_i$  and  $B_i$ . Sensitivity to the initial solution for these parameters is discussed below. All additional parameters are initialized to 0.

When measurements are taken of length and scattering parameters of a sample there exist systematic uncertainties in sample dimensional measurement, sample position measurement, and machine measurement. An orthogonal distance regression model provides the modeler with the ability to assume that the independent variable, in this case, frequency, may contain some uncertainty as well. Allowances for these types of uncertainty can, in some cases, greatly improve the approximation. For this particular model and the samples tested, the errors in the independent variables are sufficiently small that an ordinary least-squares approximation is adequate.

Model parameters such as sample length, sample position in the waveguide, and cutoff wavelength could contain a systematic uncertainty. These parameters were allowed to vary over a limited region, and the optimization procedure determines values for the parameters. This procedure assumes that systematic measurement errors can be detected by the routine. For example, inserting a sample into a sample holder introduces an uncertainty in the sample position  $L_1$ , so we include with  $L_1$  an additional optimization parameter  $\beta_{L1}$  in  $R_1$  to account for positioning uncertainties:

$$R_1 = \exp(-\gamma_o[L_1 + \beta_{L1}]). \quad (29)$$

Also for  $R_2$ :

$$R_2 = \exp(-\gamma_o[L_2 + \beta_{L2}]). \quad (30)$$

The routine requires that the length corrections be within a predescribed range which represents physical measurement uncertainty. The length of the sample  $L$  is completely determined by

$$L = L_{\text{air}} - (L_1 + L_2 + \beta_{L1} + \beta_{L2}) \quad (31)$$

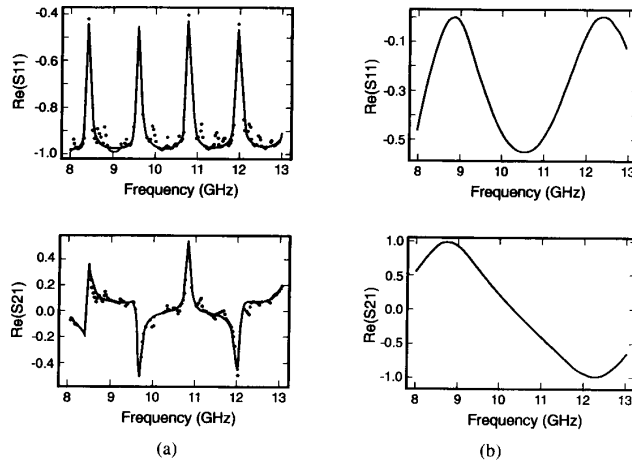


Fig. 2. Predicted (solid line) and observed (dots)  $S$ -parameters for a barium titanate compound (a) and cross-linked polystyrene in (b).

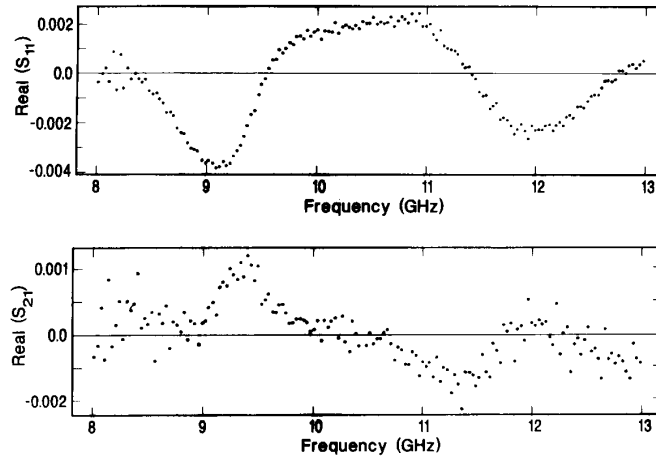


Fig. 3. Systematic uncertainty as indicated by the residual plot between the observed and predicted values for a measurement of air.

and it is also implicitly parameterized by the values of  $\beta_{L1}$  and  $\beta_{L2}$ .

Due to inaccuracies in machining of the sample holder there is an uncertainty in the cutoff wavelength of the guide. We account for this by the introduction of an additional optimization parameter  $\lambda_c \rightarrow \lambda_c + \beta_\gamma$ . We constrain this variation to be within measurement accuracy.

The model can use various combinations of the available data to estimate both the relative permeability and permittivity from scattering data. For example,  $S_{21}$  or  $S_{11}$  alone can be used to obtain both permeability and permittivity. This can be contrasted with point-by-point techniques where both  $S_{21}$  and  $S_{11}$  are required. Also, magnitude alone can similarly be used. Magnitude data have the advantage of requiring no reference plane rotation. However, there is a price for using a sparse set of constraints. This price is that the number of alternative minima increases as the constraint set decreases.

The technique works quite well for short-circuit line measurements. For short-circuit line applications it is possible with this technique to obtain both the complex permittivity and permeability from a single broadband measurement on one sample, at a single position in the line.

### B. Numerical Results

The model predictions are formed by inserting (20) and (21) or (22) into the scattering equations (10) and (12) or (16) and then finding the unknown coefficients in the equations for  $\epsilon_R^*$  and  $\mu_R^*$  that produce the least-square error. In Fig. 2 the experimental results are given for a barium titanate compound and cross-linked polystyrene. These samples required 21 and 40 iterations, respectively. The difference between the predicted  $S$ -parameter and the observed values reveals the presence of systematic uncertainty, as shown in Fig. 3. Additional tests revealed the

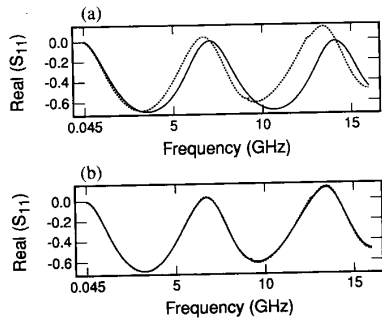


Fig. 4. Measured real part of  $S_{11}$ , measured ( $\cdots$ ) and predicted ( $\text{—}$ ), for a glass sample (a) with positioning error for  $L_1$  and (b) the solution when the algorithm adjusts for the positioning error.

source of the systematic error did not appear to be related to the material tested in the waveguide. In fact, uncertainties produced for the cross-linked polystyrene sample closely resemble the  $S$ -parameter data for an empty waveguide. We conclude therefore that much of the systematic error is due to calibration uncertainty and joint losses at connector interfaces. This was later verified when we obtained a new calibration kit and found that the systematics decreased appreciably. Note that for the barium titanate compound sample there are both the fundamental mode response and smaller resonances related to higher order modes. As shown in Fig. 2, the model interpolates a fundamental mode. This raises the possibility of extending the model to incorporate higher order modes by extending the theoretical formulation of the problem.

It is easy to move the sample in the holder inadvertently when connecting the sample holder to the port cables. Positioning errors of the sample in the air line can result in large errors in computed material parameters. The numerical algorithm can adjust for positioning errors by adjusting  $L_1$  or  $L_2$  slightly. The effects of positioning error can be seen in Fig. 4. In this example the routine predicted that the position of the sample was off by 0.8 mm.

V. PERMITTIVITY AND PERMEABILITY RESULTS

In this section we present the measured and calculated permittivity and permeability results. Cross-linked polystyrene and the barium titanate compound are nonmagnetic, and therefore  $\mu_R^* = 1$  for this problem. Comparison of the optimized solution to a point-by-point solution is shown in Fig. 5. In Figs. 6 and 7 the results for three samples are displayed. As a check we made an independent measurement of the barium titanate compound in an X-band cavity, and the results were  $\epsilon_R' = 269 \pm 5$  at 10 GHz. This result can be compared to the results in Fig. 6.

Robustness of the Procedure

Since the transmission coefficient contains a periodic component, there is more than one solution to the system of equations. Each root of the equation has a neighborhood around which convergence will occur for initial estimates in that region. The robustness of a mathematical

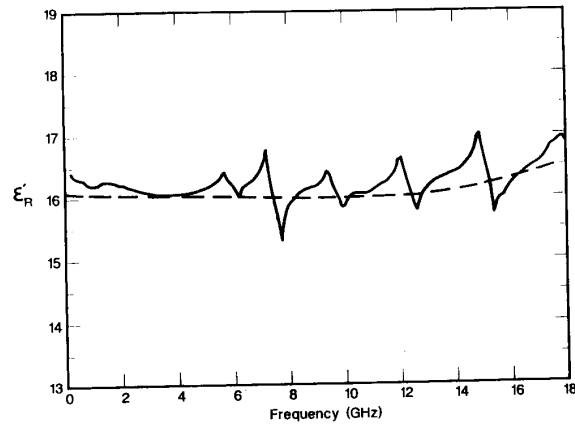


Fig. 5. Permittivity for a leaded glass over 0.045–18 GHz for the optimized solution ( $-\text{---}$ ) and point-by-point technique ( $\text{—}$ ).

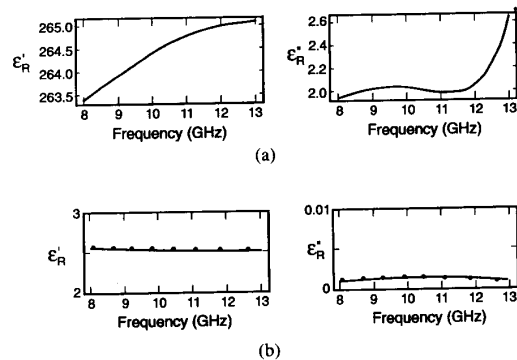


Fig. 6. Permittivity for barium titanate compound (a) and cross-linked polystyrene (b), point-by-point method ( $\cdots$ ), optimized solution ( $\text{—}$ ).

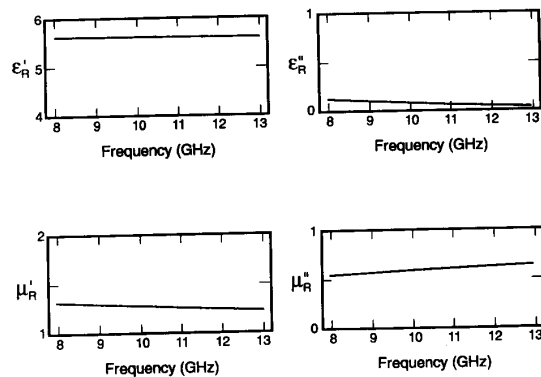


Fig. 7. Permittivity and permeability for a ferrite loaded polymer. Point-by-point method ( $\cdots$ ), optimized solution ( $\text{—}$ ).

procedure is related to how well the algorithm treats the neighborhood around the correct root. The existence of alternative optima in the mathematical model requires a reasonable initial guess (on the order of 10–20%) in order to converge to the correct solution. Typically convergence occurs after about seven iterations. The use of con-

straints and the large number of equations enhance the uniqueness of the solution by reducing the dimensions of the solution space.

The numerical effectiveness of the entire permeability and permittivity calculation depends on the robustness of the ODRPACK procedure and, more significantly, on the robustness of the mathematical model. For the materials with low dielectric constant the procedure readily determined a solution for a variety of input values with a large radius of convergence. For materials with higher dielectric constant, the procedure often converged quickly, although the existence of alternative local optima in the mathematical model required some testing to make sure that the converged root was the correct root. Group delay is a useful tool [10].

## VI. DISCUSSION

An optimization approach to the solution of the scattering equations appears to be a viable alternative to point-by-point techniques. The technique allows a stable solution for a broad range of frequencies. The method works particularly well for short-circuit line measurements. Unlike the point-by-point short-circuit method which requires measurements on two samples or in two positions, the optimized solution can obtain complex permittivity and permeability on a single sample at a single position, although the solution may exhibit some alternative minima.

The technique has been successful for many isotropic magnetic and relatively high dielectric constant materials. The reflection ( $S_{11}$ ) data are usually of lesser quality than the transmission data ( $S_{21}$ ) for low-loss, low-permittivity materials. Therefore,  $S_{11}$  need not be included in the solution for low-loss materials. However, reflection data  $S_{11}$  and  $S_{22}$  at frequencies over 1 GHz are very useful in determining the position of the sample in the air line as indicated in Fig. 7. Adding constraints to the solution is powerful in that it further limits the possible solution range of the system of equations and enhances the uniqueness of the solution. The use of analytic functions for the expansion functions allows a correlation between the real and imaginary parts of the permittivity and permeability. The results shown in Figs. 5–6 indicate that the method can be used to reduce scattering data of fairly high dielectric constant materials. In fact, we have found that in some cases the optimized procedure yields solutions when the point-by-point technique fails completely (for example the barium titanate compound in Fig. (6)).

The question arises as to why an optimization approach can, in many cases, reliably reduce data on higher dielectric constant materials ( $\epsilon'_R > 20$ ). A reason for this is that scattering data for higher dielectric materials contain responses to both primary mode and higher modes. As indicated in Fig. 2 for the barium titanate compound, the optimization routine interpolates through the primary mode data and is not unduly influenced by the higher mode resonance data.

The optimized technique can be used to treat problems where sample lengths, sample holder lengths, and sample positions are not known to high accuracy. However, in these cases there exist alternative minima. This result could find application to high-temperature measurements.

Higher order modes propagate in samples when two conditions are met. The frequencies must be above cutoff in the sample, and there must be inhomogeneities or asymmetries in the sample to excite the higher modes. Higher order modes can be incorporated into this type of model by letting the optimization routine select the power in each mode.

## REFERENCES

- [1] S. Stuchly and M. Matuszewski, "A combined total reflection transmission method in application to dielectric spectroscopy," *IEEE Trans. Instrum. Meas.*, vol. IM-27, pp. 285–288, Sept. 1978.
- [2] S. Roberts and A. von Hippel, "A new method for measuring dielectric constant and loss in the range of centimeter waves," *J. Appl. Phys.*, vol. 7, pp. 610–616, July 1946.
- [3] J. Baker-Jarvis, E. Vanzura, and W. Kissick, "Improved technique for determining complex permittivity with the transmission/reflection method," *IEEE Trans. Microwave Theory and Techniques*, vol. 38, pp. 1096–1103, Aug. 1990.
- [4] H. E. Bussey, "Measurement of rf properties of a materials survey," *Proc. IEEE*, vol. 55, pp. 1046–1053, June 1967.
- [5] G. Maze, J. L. Bonnefoy, and M. Kamarei, "Microwave measurement of the dielectric constant using a sliding short-circuited waveguide method," *Microwave Journal*, pp. 77–88, Oct. 1990.
- [6] P. D. Domich, J. Baker-Jarvis, and R. Geyer, "Optimization techniques for permittivity and permeability determination," Tech. Rep., NIST, 1991.
- [7] J. Baker-Jarvis, "Transmission/reflection and short-circuit line permittivity measurements," NIST Tech. Note 1341, National Institute of Standards and Technology, 1990.
- [8] S. R. Wallin, *Dielectric Properties of Heterogeneous Media*. Ph.D. thesis, University of Wyoming, 1985.
- [9] P. T. Boggs, J. R. Donaldson, R. H. Byrd, and R. B. Schnabel, "ALGORITHM 676 ODRPACK: software for weighted orthogonal distance regression," *ACM Transactions on Mathematical Software*, vol. 15, no. 4, pp. 348–364, 1989.
- [10] W. B. Weir, "Automatic measurement of complex dielectric constant and permeability at microwave frequencies," *Proc. IEEE*, vol. 62, pp. 33–36, Jan. 1974.